Scientific note

Ocean tides and loading in the Nordic Seas

M. S. Bos and T. F. Baker

*Proudman Oceanographic Laboratory, Bidston Observatory, Bidston Hill,
Prenton, CH43 7RA, United Kingdom (msb@pol.ac.uk)*

Abstract: A set of recent published global ocean tide models and two local ocean tide models are compared in the Nordic Seas with a set of tide gauge observations and with each other. For the M2 harmonic, a mean standard deviation of 23% was found compared with the observed tidal amplitudes. For the other constituents this number is even larger, between 34% and 51%. These differences will, to some extent, average out when the ocean loading is calculated but for the displacement ocean loading at Ny-Ålesund significantly different phase-lag values were obtained compared to those published by the International Earth Rotation Service (IERS).

1. Introduction

Several studies have compared global ocean tide models with tide gauge data and with each other within a latitude range of $-66°$ to $66°$ North (Andersen *et al.*, 1995; Shum *et al.*, 1997). This region corresponds with the coverage of the TOPEX/POSEIDON satellite from which altimetry data is assimilated in most modern ocean tide models. The ERS1/2 satellites have a higher northern latitude limit of $82°$ but so far inaccurate orbit determination has limited its use for measuring the tides. Outside this region only tide gauge observations are available and a hydrodynamic ocean tide model must be used to map the tides. Lyard (1997) extended these comparisons with his own and 2 other models over the Arctic but since then new hydrodynamic ocean tide models have been published and therefore a new comparison has been made in this paper.

Next, it is interesting to investigate if these new models produce significantly different vertical displacement ocean loading values in this area. At Ny-Ålesund and Tromsø, Very Long Baseline Interferometer (VLBI) measurements are made while at Høfn VLBI measurements have been made in the past. In addition, all three stations are equipped with Global Positioning System (GPS) receivers. Both types of instruments are capable of sub-*cm* accuracy and since ocean loading effects are of this order of magnitude the loading at these three sites will be given.

2. Description of available ocean tide models

The tides in the Nordic Seas, assumed to encompass the Norwegian Sea, Greenland Sea and the Barents Sea, are difficult to model due to lack of accurate knowledge of the

bathymetry. Furthermore, the seasonally changing ice coverage in the Arctic influences the dynamics of the tides. For the diurnal tides, there are also trapped shelf waves present which need again precise bathymetry for correct representation.

In this study eight models are used. The oldest global ocean tide model used is the Schwiderski model which is denoted as SCHW (Schwiderski, 1980). It is given on a $1° \times 1°$ grid and is included for reference purposes. Next are the two global ocean tide models ORI. 96 and NAO.99, an update of ORI.96, both given on a $0.5° \times 0.5°$ grid (Matsumoto et al., 1995, 1999).

Another set of global ocean tide models which cover the Nordic Seas are FES94.1, FES95.2 and FES98. All three are based on a finite element grid transformed to a regular latitude/longitude grid. FES94.1 and FES95.1 are given on a $0.5° \times 0.5°$ grid (Le Provost et al., 1994; Lyard, 1997), FES98 on $0.25° \times 0.25°$ (Lefèvre et al., 2000). FES94.1 is a pure hydrodynamic model while FES95.2 has assimilated TOPEX/POSEIDON data globally. Lyard then also improved the model in the Arctic. He studied the influence of ice on the tides by doubling the bottom friction coefficient over ice covered regions and found only a small influence over the deep water. More effect was observed in shallow water. FES98 assimilated tide gauge data, but not altimetry.

A local ocean tide model by Gjevik, Nøst and Straume, here after referred to as the GNS model, is given on a $0.5° \times 0.25°$ grid (Gjevik and Straume, 1989; Gjevik et al., 1994). Kowalik and Proshutinsky (1993, 1994) also developed a local ocean tide models of the Arctic and is denoted as the KP model. They model the influence of ice coverage and mention that the effect is small for the deep water.

All models capture the main features of the tides. Only the SCHW model misses the amphidrome south of Spitsbergen for the M2 harmonic. This is probably caused by the coarse grid resolution. For the semi-diurnals, the tides in the Nordic Seas are mainly driven by the tides coming from the North Atlantic Ocean which are propagating partly into the Barents Sea where they are dissipated. The rest continues through the Fram Strait into the Arctic Sea. In Fig. 2 the tidal pattern is given for the FES98 model.

The diurnal tides are driven in the same way but the influence of the gravitational potential forcing is larger. The presence of trapped waves is noticeable. See for example the Yermak plateau or the entrance to the shelf between Norway and Svalbard. The tidal pattern for the O1 harmonic can be seen in Fig. 3.

3. Comparison between tide gauges and ocean tide models

Most tide gauge data are obtained from the International Hydrographic Office and only those with a length of observation longer than 30 days were selected. Gjevik also provided tide gauge observations made in the Barents Sea. Another constraint was that all models should cover the gauges, which reduced the list to 52 gauges. Their positions are shown in Fig. 1. The White Sea has been excluded from the comparison, since the errors in this region are up to 1 m and will dominate all the other gauges. The same problem was encountered by Lyard (1997). It must be noted that the tidal amplitude is small for the diurnals making errors in the observations more significant.

The standard deviation σ between the model and the gauges was, for each harmonic, calculated with the following equation:
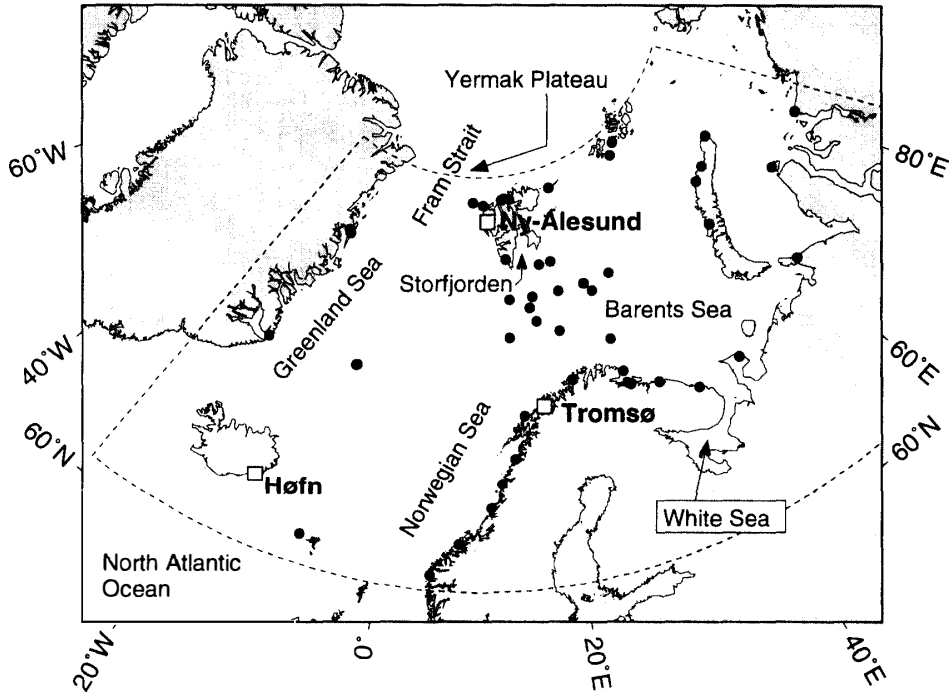
Fig. 1. *The black dots give the location of the 52 tide gauges and the white squares of the 3 VLBI/GPS stations. The dashed line indicates the region used for comparing ocean tide models.*

Table 1. *Standard deviation σ between tide gauges and ocean tide models in cm. Also the percentage of σ compared to the average amplitude of the tide at the gauges is given.*

Model	M2 cm	M2 %	S2 cm	S2 %	N2 cm	N2 %	K1 cm	K1 %	O1 cm	O1 %
FES94.1	12.71	27	7.55	44	5.54	51	4.11	58	2.39	66
FES95.2	9.32	20	5.06	30	6.10	56	2.45	34	1.76	48
FES98	9.51	20	5.43	32	3.09	29	2.30	32	1.57	43
ORI.96	10.09	22	5.02	29	3.80	35	2.97	42	2.36	65
NAO.99	8.86	19	5.60	33	4.13	38	3.00	42	1.82	50
GNS	13.19	28	5.93	35	3.11	29	2.32	33	-	-
KP	8.24	18	5.89	35	4.69	43	3.25	46	1.65	45
SCHW	12.26	26	4.91	29	4.39	40	3.14	44	1.37	38
Average	10.52	23	5.67	33	4.36	40	2.94	41	1.85	51

$$\sigma^2 = \frac{1}{N} \sum_{i=1}^{N} \frac{1}{2} \mid Z_i^{\text{gauge}} - Z_i^{\text{model}} \mid^2.$$ (1)

In this equation Z^{gauge} and Z^{model} are the tides written in complex form. This standard deviation can be interpreted as the root-mean-square of the averaged variance at each gauge. Because the variance is taken over one tidal period the factor 1/2 appears. The results are listed in Table 1.

The results for FES95.2, KP and SCHW are in good agreement with Table 4 of Lyard

Table 2.   Standard deviation σ between tide gauges and ocean tide models in cm for harmonic M2. Also the percentage of σ compared to the average amplitude of the tide at the gauges is given.

Model	Storfjorden cm	%	White Sea cm	%	South Barents cm	%
FES94.1	8.18	25	56.62	71	44.12	43
FES95.2	8.25	26	35.51	44	30.02	30
FES98	7.29	23	51.63	64	30.98	31
ORI.96	25.49	90	-	-	48.26	43
NAO.99	21.34	66	39.06	48	35.47	35
GNS	21.57	67	51.61	65	35.99	35
KP	10.20	31	31.50	41	23.39	23
SCHW	35.47	111	-	-	32.92	32

(1997). Table 1 shows that the FES94.1 model is not the most accurate model in this region. Especially for the diurnal harmonics it has a much larger σ than the other models. Overall, FES98 performs the best although not by a large margin. Part of this good fit is caused by the fact that 18 of these gauges are assimilated into FES98 which helps in lowering the standard deviation. However, with 34 non-assimilated gauges left the comparison should be fairly independent. In specific areas the errors are much larger such as in the Storfjorden (south of Spitsbergen), in the White Sea and in the south of the Barents Sea. The results of the comparisons in these areas are presented in Table 2.

4.   Differences between the FES98 and other ocean tide models

The previous section compared tide models with gauges which were mostly at the coast. Now the standard deviation will be taken between each model and FES98. If the same values are obtained then this is a good indication that the accuracy of the models within the domain is the same as at the boundary. Tide gauge comparisons can then be used as an index for the overall accuracy. The results are given in Table 3.

Table 3 shows a relatively small standard deviation of FES98-FES95.2 which is

Table 3.   The averaged standard deviation σ between the gridpoints of an ocean tide model and FES98 in cm. The area of averaging is drawn in Fig. 1. Next, the percentage of σ compared to the average amplitude of FES98 over the region is given.

Model	M2 cm	%	S2 cm	%	N2 cm	%	K1 cm	%	O1 cm	%
FES94.1	6.31	15	4.15	27	3.67	40	2.52	37	1.17	29
FES95.2	5.08	12	2.26	15	3.76	41	1.47	21	0.57	14
ORI.96	10.58	24	4.47	29	3.59	39	2.75	40	1.63	40
NAO.99	10.27	24	4.79	31	4.05	44	2.60	38	1.40	35
GNS	12.12	28	3.62	24	2.71	30	2.18	32	-	-
KP	8.29	19	3.81	25	3.71	41	2.60	38	0.88	22
SCHW	12.09	27	4.01	26	2.63	29	2.46	36	0.92	22
Average	9.25	21	3.87	25	3.45	38	2.37	35	1.04	27

FES98

FES98 - FES95.2

FES98 - NAO.99

FES98 - Schwiderski

FES98 - Kowalik

FES98 - Gjevik

| 0 | 1 | 2 | 4 | 8 | 16 | 32 | 64 | 124 |

cm
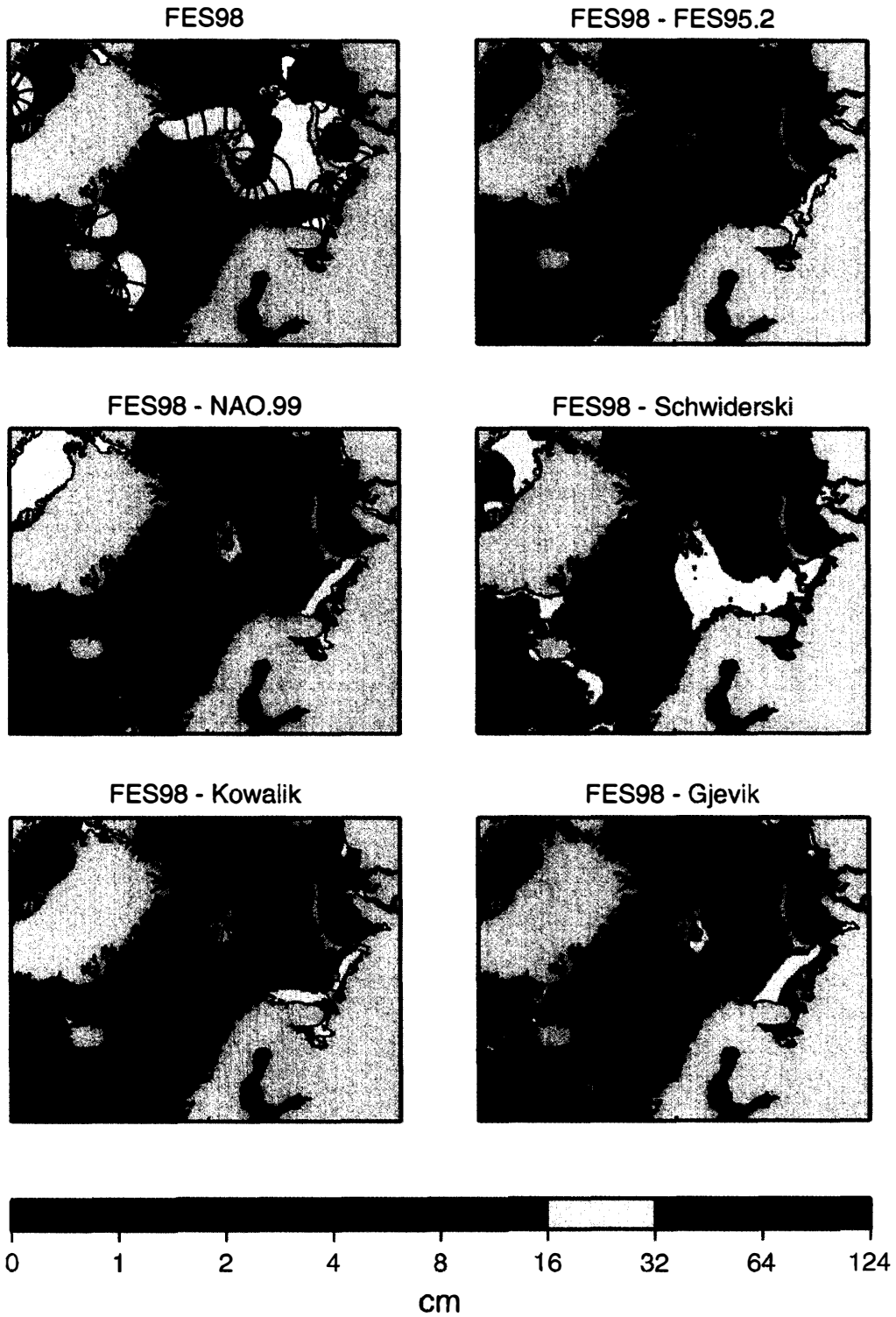
Fig. 2. The M2 tides in the Nordic Seas as given by the FES98 model and the vector difference between FES98 and 5 ocean tide models, for M2.

FES98   FES98 - FES95.2

FES98 - NAO.99   FES98 - Schwiderski

FES98 - Kowalik   FES98 - FES94.1

0.000   0.125   0.250   0.500   1.000   2.000   4.000   8.000   16.000

cm
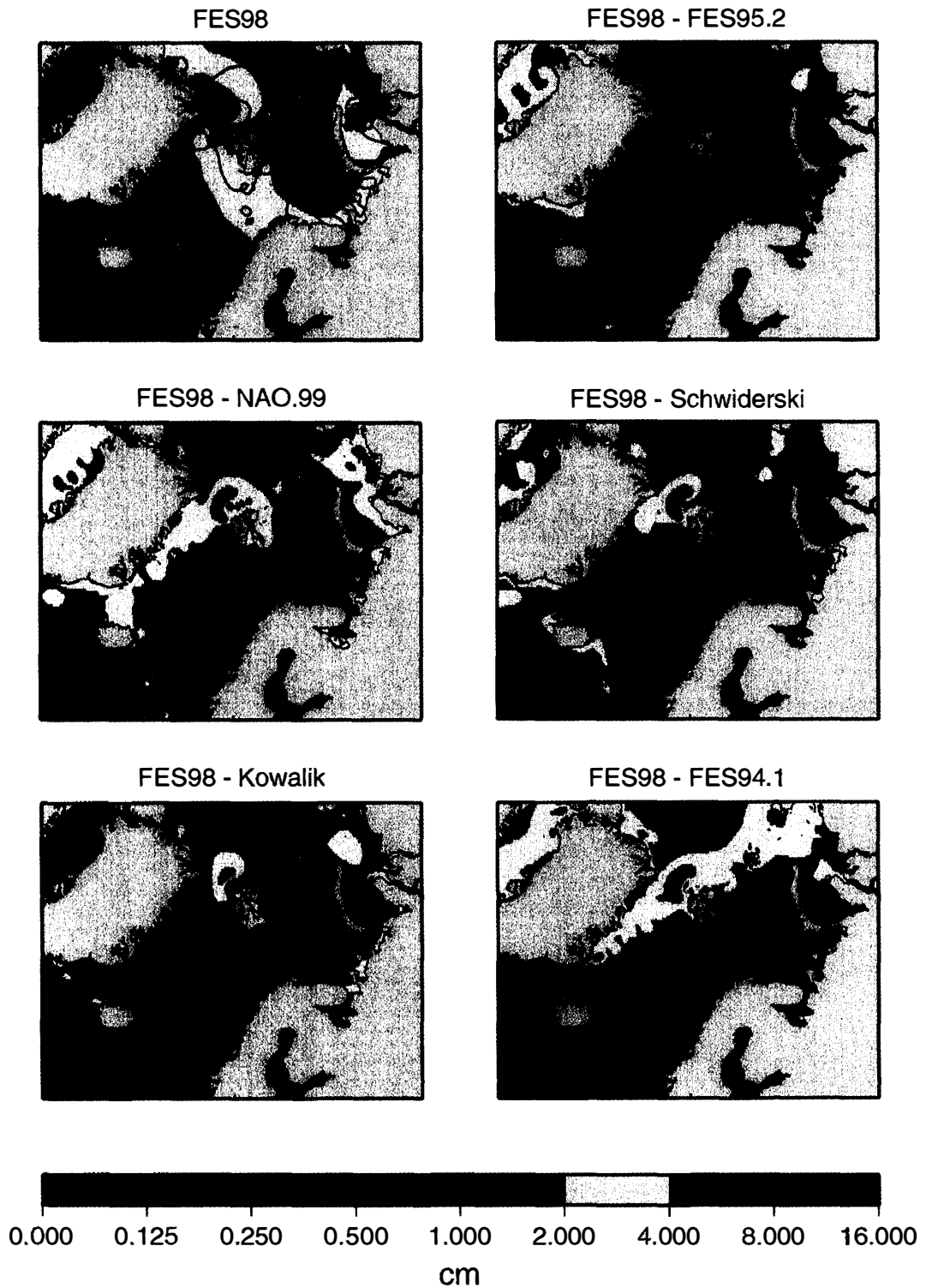
Fig. 3.   The O1 tides in the Nordic Seas as given by the FES98 model and the vector difference between FES98 and 5 ocean tide models, for O1.

understandable since these models are produced on the same finite element grid. For the diurnals the obtained values are significantly smaller than compared with the gauges. Especially the low O1 values between FES98-KP and FES98-SCHW are striking. The spatial distribution of the vector differences, $| Z^{model1} - Z^{model2} |$, is shown in Figs. 2 and 3. For harmonic M2 the large differences in the South of the Barents Sea, the White Sea and in the Storfjorden are clearly visible. The large difference of SCHW and GNS, to a lesser extent, with FES98 in the Norwegian Sea will have a large influence on the loading values at Ny-Ålesund as discussed in the next section. For harmonic O1, the most striking feature is the difference between FES98 and all models over the Yermak Plateau North of Spitsbergen.

5. Vertical ocean loading displacements

Due to the fact that the weight of the tidal water mass varies spatially with time and the elasticity of the Earth, deformations of the ocean bottom occur which are propagated to the land. For each harmonic the amount of deformation can be calculated as follows:

$$h(r) = \int_A \rho Z(r') G(| r - r' |) dA. \tag{2}$$

In this equation $h(r)$ is the vertical displacement at a specific location r, again given in its complex form. The integral is taken globally over all water masses and ρ is the mean density of sea water. Z is the complex tidal amplitude and G is a Green's function which determines how much deformation a pointload of 1 kg at a distance $| r - r' |$ causes at the station at r. For the ocean loading values presented in Table 4 the Green's function of the Preliminary Reference Earth Model is used and the tidal water mass is conserved by subtracting a uniform layer with a certain phase-lag globally from the ocean tide model. Finally, the ocean tide models are linear interpolated near the stations to a gradual refined grid to assure that the assumption of a pointload representing the continuous waterload remains valid and to improve the fit with the coastline. The finest grid size is about 50 m which is small enough since the contribution of the ocean tides within a 1 km radius around the station to the loading cannot be more than 0.14 mm for a 0.5 m tide.

The International Earth Rotation Service (IERS) also gives the vertical ocean loading displacement values for Ny-Ålesund, Tromsø and Høfn, calculated by Scherneck (McCarthy, 1996). He uses the FES94.1 model and from Table 4 one can see that the same results are obtained. It must be mentioned that the GNS and KP models were extended outside their domain with values from FES98. For Ny-Ålesund the semi-diurnal tides from the Norwegian Sea have the largest contribution to the ocean loading. From Fig. 2 one can see that for harmonic M2 the GNS and SCHW models will deviate the most from the other models. This is confirmed in Table 4. For Tromsø, the Norwegian Sea is also of importance but this station is also more influenced by tides in the North Atlantic which are more uniform between all models. At Høfn the influence of the North Atlantic is even stronger. The FES94.1 has overall a poor comparison with tide gauge observations and this shows up in Table 4 in high amplitudes for harmonics S2 and N2 and a very low amplitude for K1. The phase-lags for these three harmonics are also significantly different from the other models.

Table 4. *Vertical displacement ocean loading values for the VLBI / GPS stations. Amplitude is given in mm and the Greenwich phase lags positive.*

Ny-Ålesund, Spitsbergen

Model	M2 mm	°	S2 mm	°	N2 mm	°	K1 mm	°	O1 mm	°
Scherneck	8.37	175	3.74	−120	2.66	170	0.47	27	1.47	−109
FES94.1	8.25	175	3.71	−120	2.63	170	0.44	27	1.48	−109
FES98	8.55	180	2.94	−132	1.83	155	0.83	−40	1.94	−116
ORI.96	8.20	177	2.92	−134	1.42	154	1.02	−61	2.00	−124
NAO.99	7.44	178	2.45	−145	1.19	151	1.02	−43	1.85	−125
GNS	9.24	168	3.25	−144	2.03	159	1.32	−33	-	-
KP	8.60	182	3.37	−139	2.15	160	0.68	−74	1.93	−125
SCHW	8.62	204	3.24	−116	1.77	180	1.43	−20	1.66	−121

Tromsø, Norway

Model	M2 mm	°	S2 mm	°	N2 mm	°	K1 mm	°	O1 mm	°
Scherneck	9.50	169	4.43	−141	3.31	148	2.38	−18	2.06	−107
FES94.1	9.76	169	4.55	−141	3.41	147	2.43	−17	2.09	−107
FES98	10.01	174	3.43	−143	2.20	148	2.37	−32	2.23	−115
NAO.99	10.15	174	3.18	−150	1.73	152	2.27	−29	2.26	−115
SCHW	11.67	192	4.10	−134	2.33	160	2.48	−17	1.88	−115

Høfn, Iceland

Model	M2 mm	°	S2 mm	°	N2 mm	°	K1 mm	°	O1 mm	°
Scherneck	11.64	−16	4.78	16	2.15	−39	5.56	−50	3.30	−110
FES94.1	11.48	−16	4.75	16	2.10	−39	5.60	−50	3.36	−110
FES98	11.97	−19	4.96	18	2.30	−42	5.58	−50	3.23	−113
NAO.99	11.98	−17	4.82	22	2.43	−39	5.56	−51	3.41	−109
SCHW	12.26	−23	4.82	29	2.53	−29	5.22	−43	2.92	−117

6. Conclusions

It has been shown that the mean standard deviation in ocean tide models of the Nordic seas for the M2 harmonic is 23% compared with the average amplitude at the tide gauges. For the other harmonics this error is even larger. Problem areas are the Storfjorden, the White Sea and the South of the Barents Sea. Comparisons with the tide gauges have also shown that FES94.1 and SCHW models perform worse than the other models. Especially for the K1 harmonic, FES94.1 has a large standard deviation which shows up as a very different phase-lag of the vertical ocean loading displacement value at Ny-Ålesund. Overall, the ocean loading amplitude values obtained are quite similar for all ocean tide models and their difference will mainly be measurable by their different phase-lags. For loading the most important errors are caused by relatively small errors in the amplitude and phase-lag in the Norwegian Sea because this region is coherent in phase for the semi-diurnal tides causing a large loading effect.

Acknowledgments

References

Andersen, O.B., Woodworth, P.L. and Flather, R.A. (1995): Intercomparison of recent ocean tide models. J. Geophys. Res., **100**, 25261–25282.

Gjevik, B. and Straume, T. (1989): Model simulations of the M2 and the K1 tide in the Nordic Seas and Arctic Ocean. Tellus, **41A**, 73–96.

Gjevik, B., Nost, E. and Straume, T. (1994): Model simulations of the tides in the Barents Sea. J. Geophys. Res., **99**, 3337–3350.

Kowalik, Z. and Proshutinsky, A.Y. (1993): Diurnal Tides in the Arctic Ocean. J. Geophys. Res., **98**, 16449–16468.

Kowalik, Z. and Proshutinsky, A.Y. (1994): The Arctic Ocean tides. The Polar Oceans and Their Role in Shaping the Global Environment, ed. by O. Johannessen *et al.* Washington, D.C., Am. Geophys. Union, 137–158 (Geophysical Monograph Vol. 85).

Le Provost, C., Genco, M.L., Lyard, F., Vincent, P. and Canceil, P. (1994): Spectroscopy of the world ocean tides from a finite-element hydrodynamic model. J. Geophys. Res., **99**, 24777–24797.

Lefèvre, F., Lyard, F.H. and Le Provost, C. (2000): FES98: A new global tide finite element solution independent of altimetry. Geophys. Res. Lett., **27**, 2717–2720.

Lyard, F.H. (1997): The Tides in the Arctic Ocean from a finite element model. J. Geophys. Res., **102**, 11611–15638.

Matsumoto, K., Ooe, M., Sato, T. and Segawa, J. (1995): Ocean tide model obtained from TOPEX/POSEIDON altimetry data. J. Geophys. Res., **100**, 25319–25330.

Matsumoto, K., Takanezawa T., Sato, T. and Ooe, M. (1999): NAO.99 Tidal Prediction System. TOPEX/POSEIDON and Jason-1 Science Working Team Meeting, Saint-Rapaël (abstract), 8.

McCarthy, D.D., ed. (1996): IERS Technical Note 21. Observatoire de Paris.

Schwiderski, E.W. (1980): On charting global ocean tides. Rev. Geophys. Space Phys., **18**, 243–268.

Shum, C.K., Woodworth, P.L., Andersen, O.B., Egbert, G.D., Francis, O., King, C., Klosko, S.M., Le Provost, C., Li, X., Molines, J.M., Parke, M.E., Ray, R.D., Schlax, M.L., Stammer, D., Tierney, C.C., Vincent, P. and Wunch, C.I. (1997): Accuracy assesment of recent ocean tide models. J. Geophys. Res., **102**, 25173–25194.